

© Copyright 2008 American Meteorological Society (AMS). Permission to use figures, tables, and brief excerpts from this work in scientific and educational works is hereby granted provided that the source is acknowledged. Any use of material in this work that is determined to be “fair use” under Section 107 of the U.S. Copyright Act or that satisfies the conditions specified in Section 108 of the U.S. Copyright Act (17 USC §108, as revised by P.L. 94-553) does not require the AMS’s permission. Republication, systematic reproduction, posting in electronic form on servers, or other uses of this material, except as exempted by the above statement, requires written permission or a license from the AMS. Additional details are provided in the AMS CopyrightPolicy, available on the AMS Web site located at (<http://www.ametsoc.org/AMS>) or from the AMS at 617-227-2425 or [copyright@ametsoc.org](mailto:copyright@ametsoc.org).

Permission to place a copy of this work on this server has been provided by the AMS. The AMS does not guarantee that the copy provided here is an accurate copy of the published work.

## 12.3 IMPROVING WEATHER RADAR DATA QUALITY FOR AVIATION WEATHER NEEDS\*

David J. Smalley<sup>†</sup>

Evelyn Mann

Chuck Ivaldi

Betty J. Bennett

Massachusetts Institute of Technology, Lincoln Laboratory

### 1. INTRODUCTION

A fundamental function of any aviation weather system is to provide accurate and timely weather information tailored to the specific air traffic situations for which a system is designed. Weather location and intensity are of prime importance to such systems. Knowledge of the weather provides “nowcasting” functionality in the terminal and en route air spaces. It also is used as input into aviation weather forecasting applications for purposes such as storm tracking, storm growth and decay trends, and convective initiation.

Weather radar products are the primary source of the weather location and intensity information used by the aviation weather systems. In the United States, the primary radar sources are the Terminal Doppler Weather Radar (TDWR) and the Weather Surveillance Radar 1988 Doppler (WSR-88D, known as NEXRAD). Additional weather radar products from the Canadian network are used by some of the aviation weather systems. Product quality from all these radars directly impacts the quality of the down stream products created by the aviation weather systems and their utility to air traffic controllers.

Four FAA weather systems use some combination of products from the aforementioned radars. They are the Corridor Integrated Weather System (CIWS), the Integrated Terminal Weather System (ITWS), the Weather and Radar Processor (WARP), and the Medium Intensity Airport Weather System (MIAWS). This paper focuses on the improvement of weather radar data quality specific to CIWS. The other mentioned FAA aviation weather systems also benefit either directly or indirectly from the improvements noted in this paper.

For CIWS, the legacy data quality practices involve two steps. Step one is the creation of weather radar products of highest possible fidelity. The second step involves creating a mosaic from these products. The mosaic creation process takes advantage of inter-radar product comparisons to interject a further level of improved data quality. The new CIWS data quality plan will use a mounting evidence data quality classifier technique currently being developed. The technique applies a multi-tiered approach to weather radar data quality. Its premise is that no single data quality improvement technique is as effective as a collaboration of many. The evidence will be expanded to include data and products from the radars along with data from additional sensing platforms. The mosaic creation process will correspondingly expand to take advantage of the additional evidence. Section 2 covers data quality of products from the single radar perspective. Section 3 focuses on the use of satellite data as the first additional sensing platform to augment removal of problematic radar contamination. Section 4 describes the data quality procedures associated with creation of mosaics from the single radar products augmented with new satellite masking information. Last, Section 5 discusses future plans for the mounting evidence data quality improvement technique.

### 2. SINGLE RADAR DATA QUALITY

There are two opportunities to improve the data quality of single-radar products. Both aim to provide data of the highest quality possible to the algorithms that generate radar products. The first opportunity to improve data quality occurs with the actual operation of the radar. Sophisticated radar engineering techniques are used in the collection of the radar I/Q data and its conversion to the primary radar moments. New engineering techniques are being developed and deployed to the TDWRs and NEXRADs for this purpose. The second opportunity to improve single-radar data quality occurs through post-collection analysis of the radar moments. If necessary, residual contaminants in the radar data can be at least

---

\* This work was sponsored by the Federal Aviation Administration (FAA) under Air Force Contract FA8721-05-C-0002. Opinions, interpretations, conclusions, and recommendations are those of the authors and are not necessarily endorsed by the United States Government.

<sup>†</sup>Corresponding author address: David Smalley, MIT Lincoln Laboratory, 244 Wood Street, Lexington, MA 02420-9185; e-mail: [daves@ll.mit.edu](mailto:daves@ll.mit.edu)

partially mitigated before use by product-generating algorithms.

The post-collection analysis is discussed for this paper. The NEXRAD Data Quality Assurance (DQA) algorithm is used to improve post-collection NEXRAD data quality for FAA applications (Smalley and Bennett, 2002). The DQA algorithm as originally developed has two data quality editing modules. The first identifies and removes constant power functions (CPFs). The second identifies and removes anomalous propagation (AP) clutter. CPFs appear in the data as steadily increasing reflectivity with range along a radial. They are caused by radar component failure, interference, and the sun. AP in the data is noted as relatively high reflectivity associated with near-zero Doppler data (radial velocity and spectrum width). In both cases, true weather returns may present in the data with similar signatures. This is particularly the case concerning weather returns in the radial velocity zero isodop region. Both editing modules attempt to effectively remove the contaminant data while not removing actual weather returns.

The edited reflectivity data from the DQA is used as input to the NEXRAD High Resolution Vertically Integrated Liquid (HRVIL) algorithm and the High Resolution Enhanced Echo Tops (HREET) algorithm (Smalley *et al.*, 2003). The three algorithms were developed by MIT/Lincoln Laboratory specifically to yield products used by FAA aviation weather systems. DQA was

released to the operational NEXRAD network in March 2003 as part of the open Build 3 providing data input to the HRVIL algorithm that preceded it. HREET was operationally deployed in September 2003 with open Build 4 and also required input data from the DQA algorithm. The HRVIL and HREET products are used in the mosaic creation step to yield the CIWS domain graphics.

While the quality of the HRVIL and HREET products is improved through the original DQA, data quality issues persist. On occasion when the HRVIL and/or HREET quality is degraded, downstream aviation weather system processes such as the mosaic step and forecast algorithms are negatively impacted. Two stop gap improvements will be operationally deployed with open build 10 (spring 2008). The Build 10 DQA algorithm is upgraded to specifically remove CPFs caused by solar interference that are interlaced with weather. The original DQA algorithm removed CPFs (including those of solar origin) only when not interlaced with weather signature. The upgrade will remove the solar CPF while retaining the weather signature since solar CPFs are predictable and their power is much weaker than any important weather signatures. Figure 1 illustrates the effect of this DQA upgrade on the HRVIL product. The left image shows a sunset stroke remaining in the product since at close range strong weather returns are present. On the right, the stroke has been removed while retaining the weather.

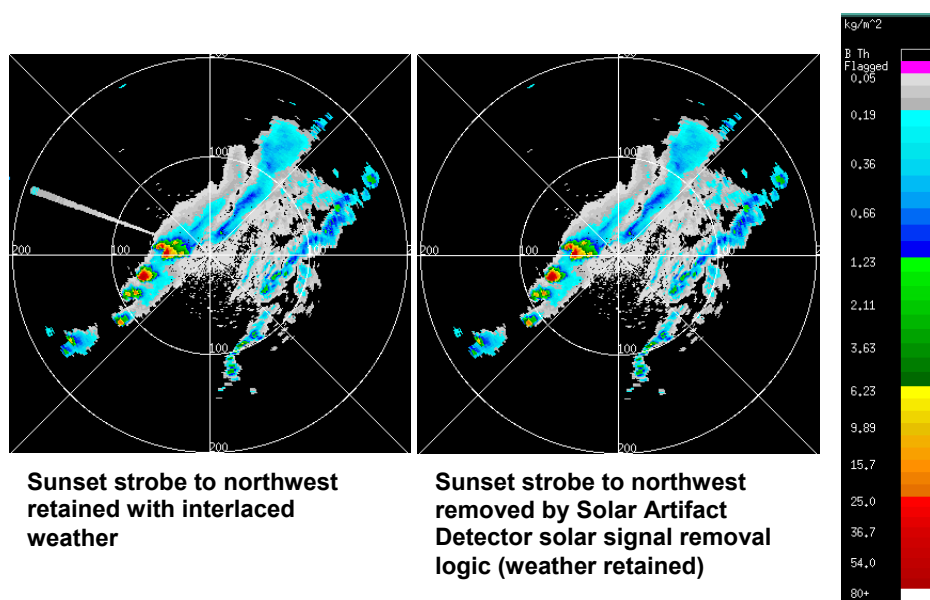


Figure 1. Example of a HRVIL product with sunset stroke breakthrough (gray/blue spoke in left image) and its resultant removal (right) from the KFWS (Forth Worth, TX) NEXRAD on May 9, 2002 at 0106 UTC.

In Build 10, HREET will be upgraded to mitigate the occurrence of high altitude spurious echo top points. These points erroneously suggest areas to avoid en route. These points are defined as being isolated and meteorologically implausible with an echo top (18 dBZ or greater) of at least 45 kft without any reflectivity below that altitude. In monitoring nine NEXRAD sites during two consecutive weeks in April 2006, on average 134 HREET products per day were contaminated with spurious points. Projecting that rate for the entire NEXRAD network predicts about 2000 contaminated HREET products per day. Figure 2 illustrates the concept applied to the HREET product. On the left, a spurious echo top point of 62 kft to the northwest at 210 km range is identified (inside red circle). On the right, the point has been removed by the new Build 10 logic.

Additional classes of radar contaminants in the HRVIL and HREET products are being addressed with open Build 11 (spring 2009). Figure 3 illustrates a selection of HRVIL and HREET products contaminated with spikes or speckle. These contaminants are caused by radar

component degradation and outside interference. The Build 11 DQA algorithm will incorporate an additional editor to identify and remove spikes and speckle.

The spike editor adopts the National Severe Storms Laboratory (NSSL) technique for spike editing (Howard, personal communication). A spike along a radial is defined as a sequence of a minimum ten consecutive range gates (10 km range) all with reflectivity. Additionally, the corresponding range gates of the two adjacent radials must be mainly devoid of reflectivity. Figure 4 shows the NSSL logic described in detail with their sequence defined as 5 range gates. The speckle editor applies a 5x5 kernel centered on a target range gate (see Figure 5). The editor removes the target (blue cell) when it has reflectivity while at least 75 percent of the neighboring range gates are devoid of reflectivity. The kernel is applied in three successive passes to account for circumstances of dense NEXRAD speckle. The set of images in Figure 5 show speckle in the reflectivity data that will be removed with the speckle editor.

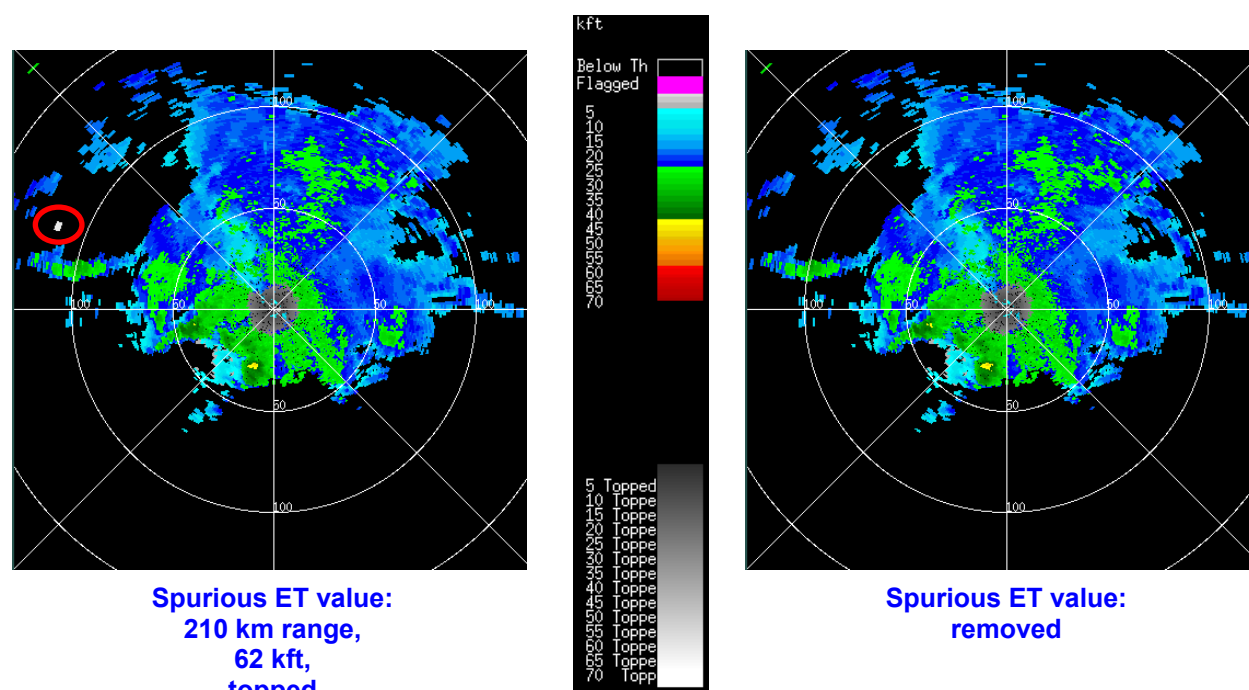


Figure 2. An identified spurious echo top value (circled in red) in the HREET product (left) from the KFWS (Fort Worth, TX) NEXRAD on March 18, 2006 at 1731 UTC. On the right is the resultant Build 10 HREET product with the point removed by the upgraded algorithm logic.

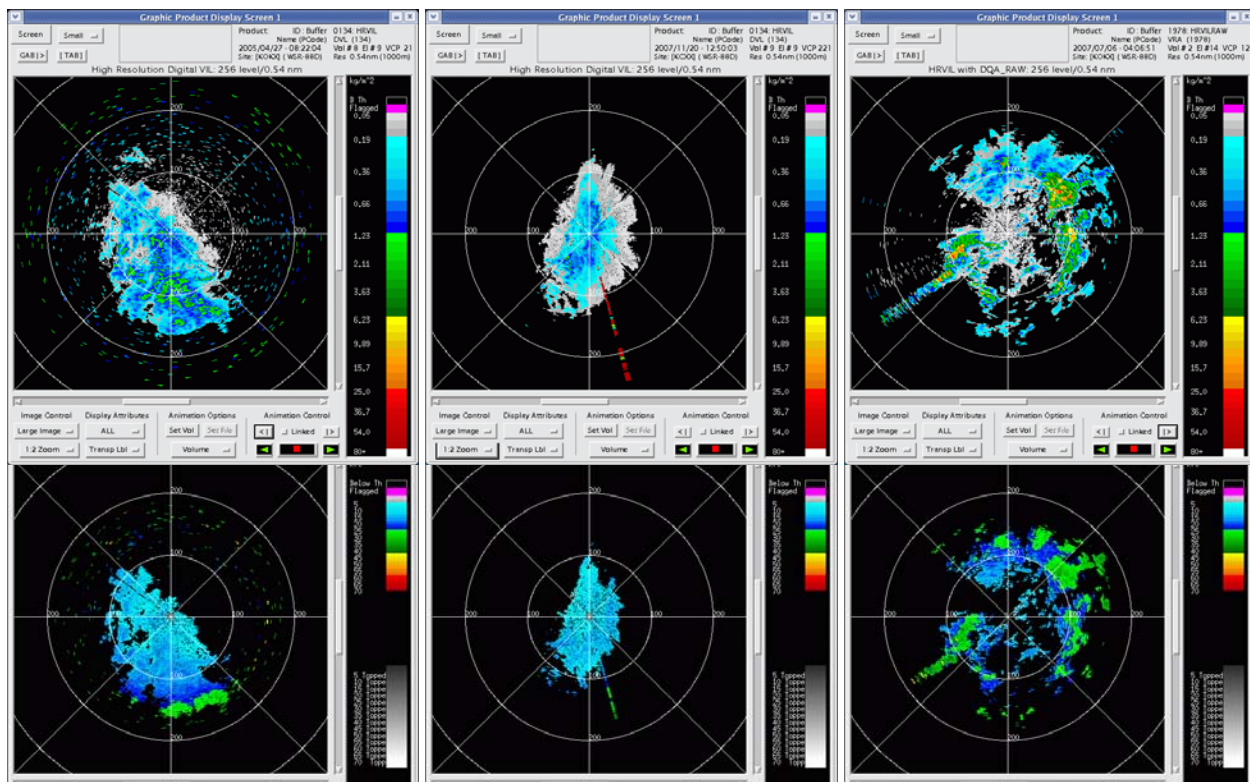


Figure 3. There are additional spike and speckle data quality problems to be dealt with as seen in these examples of HRVIL (upper images) and HREET (lower images). For NEXRAD Build 11, a spike and speckle quality editor will be added to mitigate such contamination.

## Spike Removal Logic

- For any given pixel with non-missing reflectivity value
  - Count the number (N1) of contiguous neighboring pixels with non-missing value along azimuth direction on both side of the given pixel.
  - Check the differences of the N1 numbers between five or more continuous pixels along radial direction.
  - If all N1s  $\leq 3$  and all the differences  $\leq 1$ , then the five or more contiguous pixels are considered a non-meteorological spike and are removed.

Courtesy of Ken Howard, NSSL

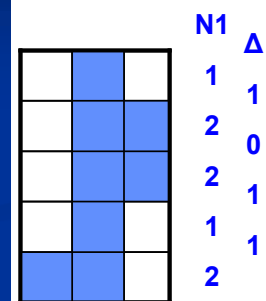


Figure 4. NSSL spike identification logic used as a basis for implementation into DQA.



- **Identifies isolated sample volumes in a 5 azimuth by 5 gate kernel**
  - Target removal if at least 75% of neighbors are without return
- **Three passes with removal after each pass**
  - Texture of NEXRAD speckle tends to be dense

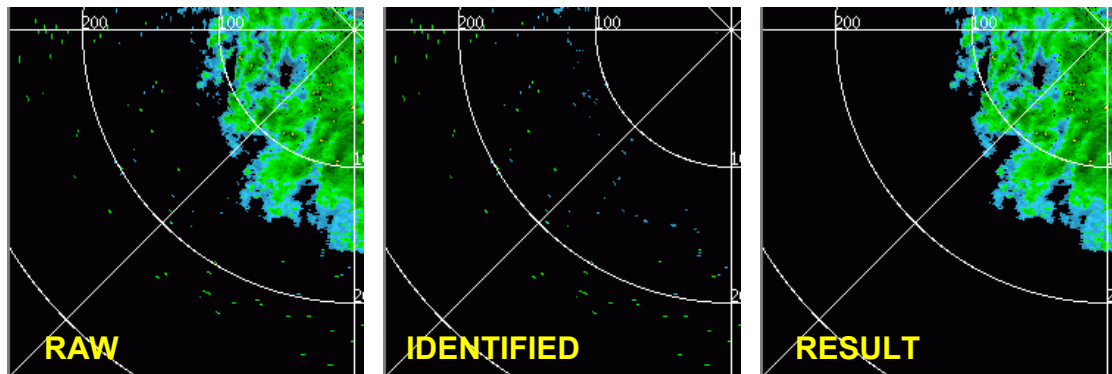
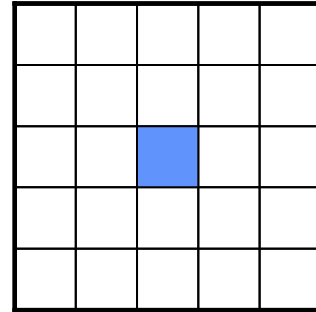


Figure 5. The spike editor 5x5 kernel and sample result. See the text for further detail.

Figure 6a-d shows a sequence of images for two cases illustrating the benefit of the spike and speckle editor. Figure 6a shows HREET with a spike to the southeast removed (along with some speckle). The upper left shows the delta echo top value between the HREET products from Build 10 (B10 on right) and Build 11 (B11 on right). The lower left histogram shows the distribution of echo tops between the two builds. The overall character of the products' echo top distributions remains the same but the erroneous high echo tops associated with the spike have been removed. Figure 6b, for the same case, shows the HRVIL transition depicted in a similar manner. The histogram verifies the product distributions are qualitatively the same. Since HRVIL is a vertical integration of estimated liquid water, the impact of the speckle editor is to slightly reduce HRVIL where speckle is removed at the edge of individual tilts. At higher tilt elevation angles of a radar volume, those removed speckle edges are increasingly closer to the radar location. This is seen as somewhat concentric magenta rings denoting VIL reduced by 1 digital scale value. The spike with its very high VIL is removed. Figures 6c and 6d show a similar analysis regarding a case dominated by speckle in many of the tilts of the

radar volume. The fidelity of the weather signatures of HRVIL and HREET are apparent between the two builds.

Improving the quality of HRVIL and HREET products from the single NEXRAD radars is the first step toward providing CIWS and the other FAA aviation weather systems with high fidelity weather location and intensity information. Remaining data quality problems with these products can be mitigated by utilizing the mounting evidence classifier technique during the per-radar processing and mosaic creation steps. In particular, strong radar echoes from biological targets during the warm season are problematic. The echoes occur especially in fair weather starting a bit before dusk and ending a bit after dawn. During strong inversions, the temporal extent of the problem worsens. Usually an entire region of radars exhibit the problem returns. The echoes are associated with motion causing the AP editor not to remove them. The mosaic creation process also struggles during regional outbreaks. CIWS has begun to incorporate satellite data in the mounting evidence paradigm. One of the first objectives is to use a satellite mask to identify areas in single-radar products that may be observing fair weather biological returns.

## NET CHANGE WITH PROPOSED B11 DQA

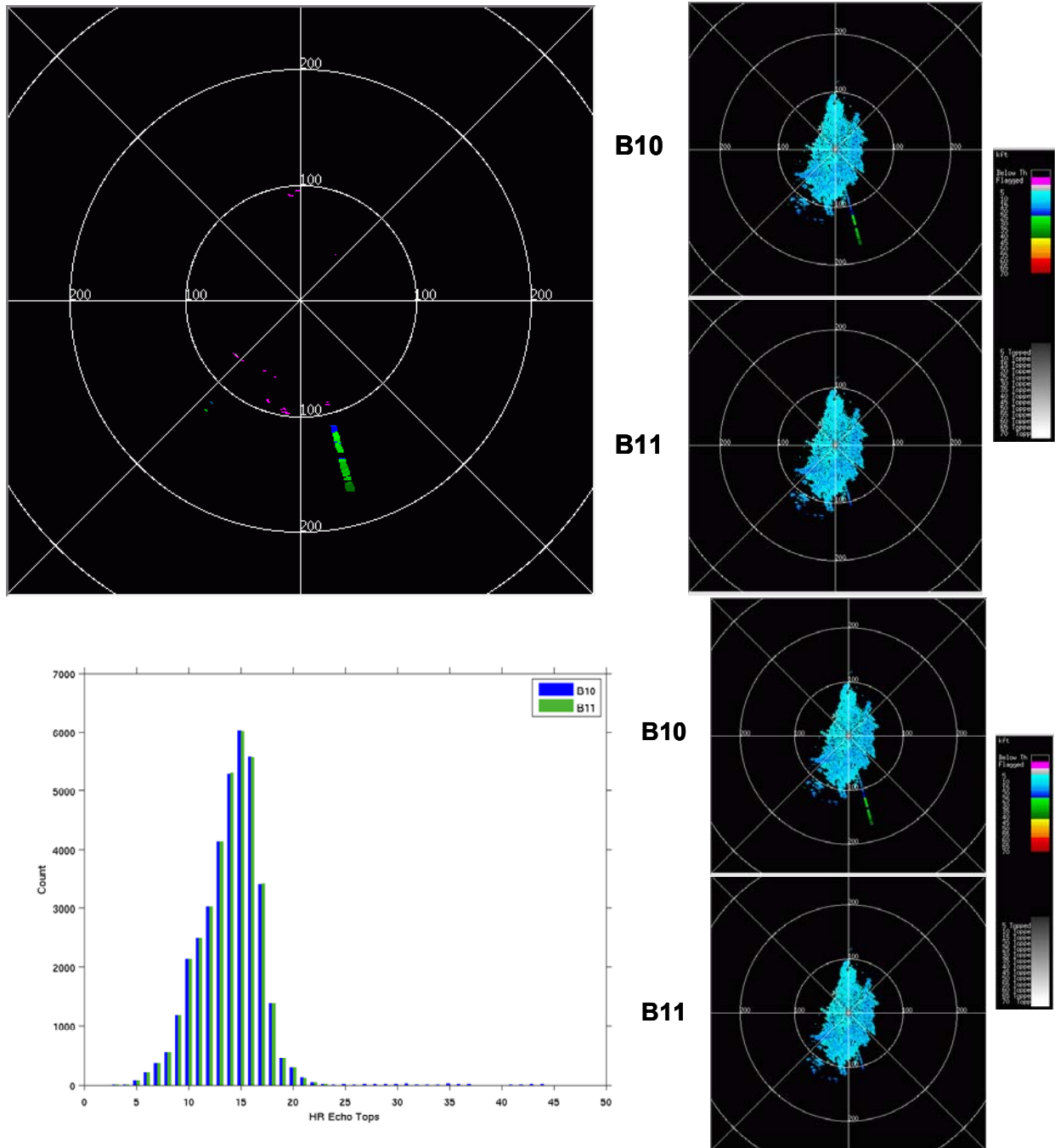


Figure 6a. The effect on HREET of the spike removal logic for the Build 11 DQA algorithm for the KCXX (Burlington, VT) NEXRAD on November 20, 2007 at 1250 UTC. The plan view (upper left) shows the net change in echo top values. The histogram shows the before (B10) and after (B11) distribution of echo tops for the right side images.

## NET CHANGE WITH PROPOSED B11 DQA

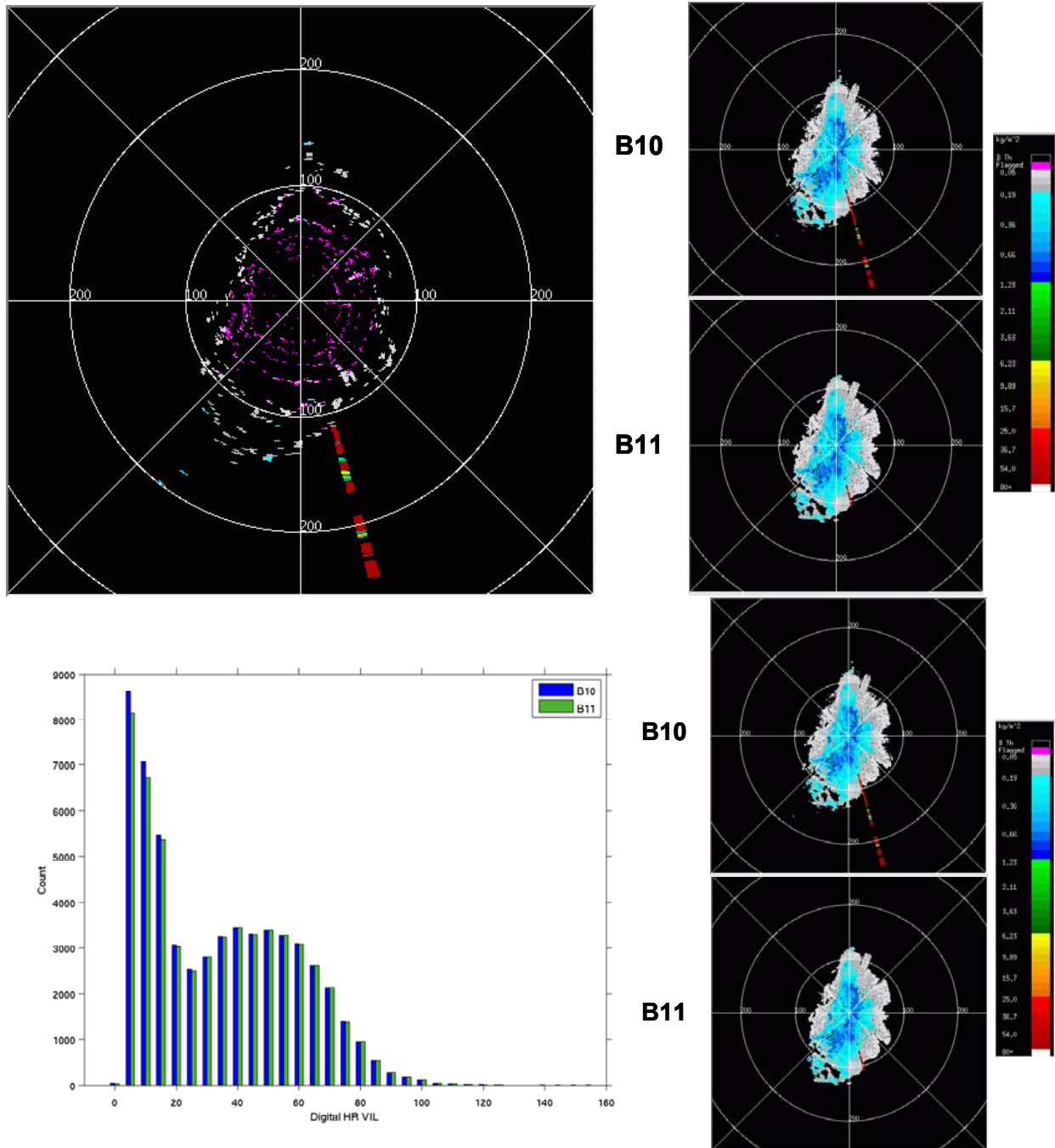


Figure 6b. The effect on HRVIL of the spike removal logic for the Build 11 DQA algorithm for the KCXX (Burlington, VT) NEXRAD on November 20, 2007 at 1250 UTC. The plan view (upper left) shows the net change in HRVIL values. The histogram shows the before (B10) and after (B11) distribution of HRVIL for the right side images.



## NET CHANGE WITH PROPOSED B11 DQA

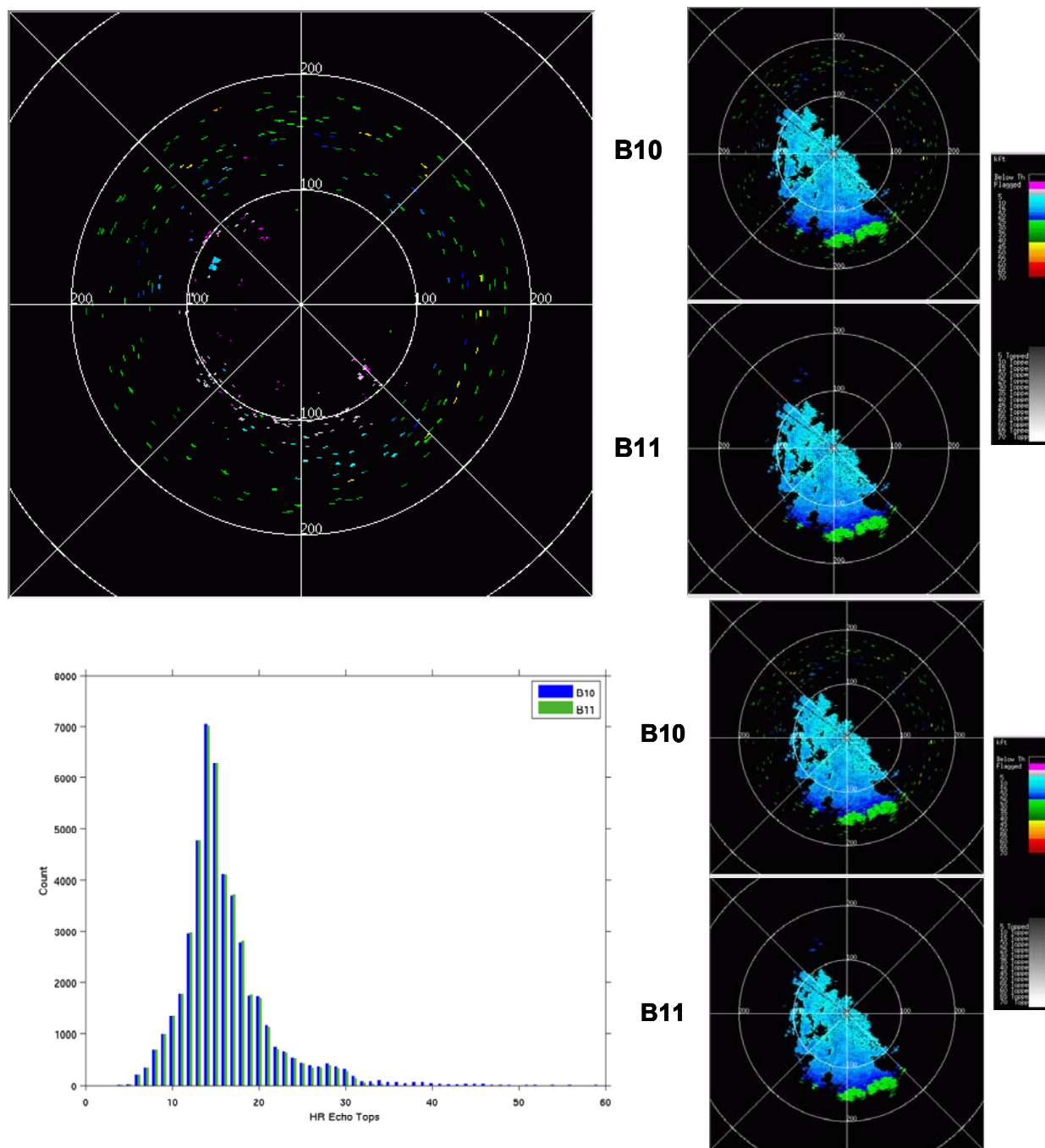


Figure 6c. The effect on HREET of the spike removal logic for the Build 11 DQA algorithm for the KOKX (Brookhaven, NY) NEXRAD on April 27, 2005 at 0822 UTC. The plan view (upper left) shows the net change in echo top values. The histogram shows the before (B10) and after (B11) distribution of echo tops for the right side images.

## NET CHANGE WITH PROPOSED B11 DQA

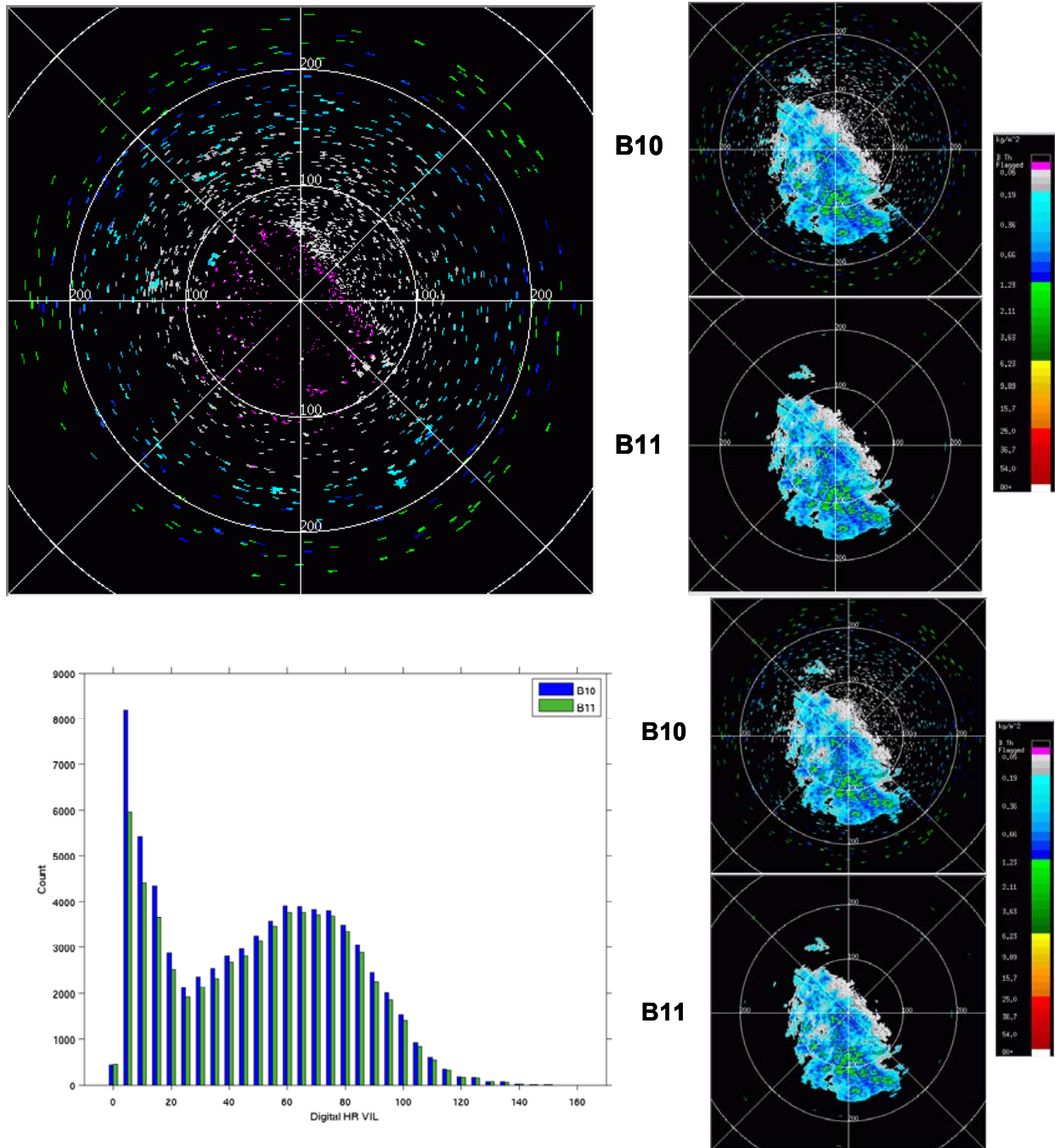


Figure 6d. The effect on HRVIL of the spike removal logic for the Build 11 DQA algorithm for the KOKX (Brookhaven, NY) NEXRAD on April 27, 2005 at 0822 UTC. The plan view (upper left) shows the net change in HRVIL values. The histogram shows the before (B10) and after (B11) distribution of HRVIL for the right side images.

### 3. INCORPORATION OF SATELLITE

The satellite cloud mask utilized in the data quality editing step for individual radar products is an adaptation of two existing cloud detection techniques. The first was developed at NASA/MSFC Global Hydrology and Climate Center (GHCC) (Jedlovec and Laws, 2003) as part of a program known as the Short-term Prediction and Research Transition (SPoRT). The program's goal is to infuse products developed from NOAA and NASA research into NWS forecast operations and decision-making at regional and local levels. A derivative of this technique is also utilized by the FAA's Aviation Weather Research Program's National Ceiling and Visibility Research Team to detect cloud-free conditions in areas not covered by surface reports. The algorithm employs a bi-spectral threshold technique using mid- and long-wave window IR (infrared) channel differences to discern cloud from clear areas. The bi-spectral threshold technique requires characterization of the background, utilizing a multi-day (the MIT/LL implementation uses 15 days) rotating archive of hourly minimum channel differences, both positive and negative, to generate composite images that provide dynamic thresholds that vary both spatially and temporally. The bi-spectral method does not use the visible channel so algorithm tests are the same for day and night. An additional 15-day rotating archive of hourly maximum (warmest) brightness temperatures from the IR window channel and minimum (darkest) albedo values from the visible channel used to generate composite images supports additional threshold tests to detect obvious cold cloud and obvious bright cloud (daytime only).

The second cloud detection technique is from the Support of Environmental Requirements for Cloud Analysis and Archive (SERCAA) program, in which cloud analysis algorithms for both polar-orbiting and geostationary weather satellites were developed to support climate and global change studies (Gustafson et al., 1994 and d'Entremont and Gustafson, 2003). These algorithms were also selected by the United States Air Force as part of their modernization program, known as the Cloud Depiction and Forecast System II (CDFS II), to provide improved global cloud analysis and forecast products in support of combat operations and planning. The geostationary algorithm uses a hybrid approach to detect cloud consisting of a temporal differencing test, coupled with a dynamic thresholding test, and various non-temporal spectral discriminant tests. The tests are designed to run with the data that are available; so, visible and IR data are used during daylight hours with only IR at night. Of the tests that comprise the SERCAA algorithm, the MIT/LL cloud detection algorithm implements some of the non-temporal spectral discriminant tests and utilizes the dynamic thresholding test separate from temporal differencing to address deficiencies in winter nighttime detection of low cloud.

Table 1 summarizes the tests used from SPoRT and SERCAA that comprise the MIT/LL cloud detection algorithm. Details of each of the tests can be found in the references cited above. Figure 7 is an example of the product produced by the MIT/LL cloud detection algorithm (cloud mask) and Figure 8 is the concomitant visible imagery from GOES-12.

**Table 1. Spectral discriminant tests that comprise the MIT/LL cloud detection algorithm.**

Test	Day	Night	Inferred Cloud Type	Comments	Source
$(T_{3.9} - T_{10.7}) - T_{MN} > \Omega_{DAY}$	√				SPoRT
$(T_{10.7} - T_{3.9}) - T_{MP} > \Omega_{NIGHT}$		√			SPoRT
$TB_{10.7} - T_{10.7} > \Omega_{COLD}$	√	√	Obvious cold cloud		SPoRT/ SERCAA
$V - VB > \Omega_{BRIGHT}$	√		Obvious bright cloud		SERCAA
$T_{3.9} - T_{10.7} > \Omega_{LC_{DAY}}$ and $TB_{10.7} - T_{10.7} < \Omega_{LC_{IR}}$	√		Low cloud, fog and stratus	Second test ensures cloud temperature is close to the underlying surface.	SERCAA
$T_{3.9} - T_{10.7} > \Omega_{CB}$ and $TB_{10.7} - T_{10.7} > \Omega_{CB_{IR}}$ and $V / \cos\theta > \Omega_{CB_{VIS}}$	√		Cb and optically thick cirrostratus	Second test ensures the cloud is cold.  Third test ensures the cloud is bright.	SERCAA
$T_{10.7} - T_{3.9} > \Omega_{LC_{NIGHT}}$		√	Low cloud, fog and stratus		SERCAA
$T_{3.9} - T_{10.7} > \Omega_{CI}$		√	Thin cirrus		SERCAA
V	GOES visible channel albedo				
$T_{3.9}$	GOES midwave brightness temperature				
$T_{10.7}$	GOES longwave brightness temperature				
$T_{MN}$	smallest negative difference (LWIR-MWIR composite)				
$T_{MP}$	smallest positive difference (LWIR-MWIR composite)				
TB	thermal background (LWIR composite)				
VB	visible background albedo (Visible composite)				
$\Omega_{DAY}$	daytime bi-spectral threshold				
$\Omega_{NIGHT}$	nighttime bi-spectral threshold				
$\Omega_{COLD}$	cold cloud threshold				
$\Omega_{BRIGHT}$	bright cloud threshold				
$\Omega_{LC_{DAY}}$	daytime bi-spectral low-cloud threshold				
$\Omega_{LC_{NIGHT}}$	nighttime bi-spectral low-cloud threshold				
$\Omega_{LC_{IR}}$	daytime thermal low-cloud threshold				
$\Omega_{CB}$	daytime bi-spectral Cb threshold				
$\Omega_{CB_{IR}}$	daytime thermal Cb threshold				
$\Omega_{CB_{VIS}}$	daytime visible Cb threshold				
$\Omega_{CI}$	nighttime bi-spectral Ci threshold				
$\theta$	solar zenith angle				

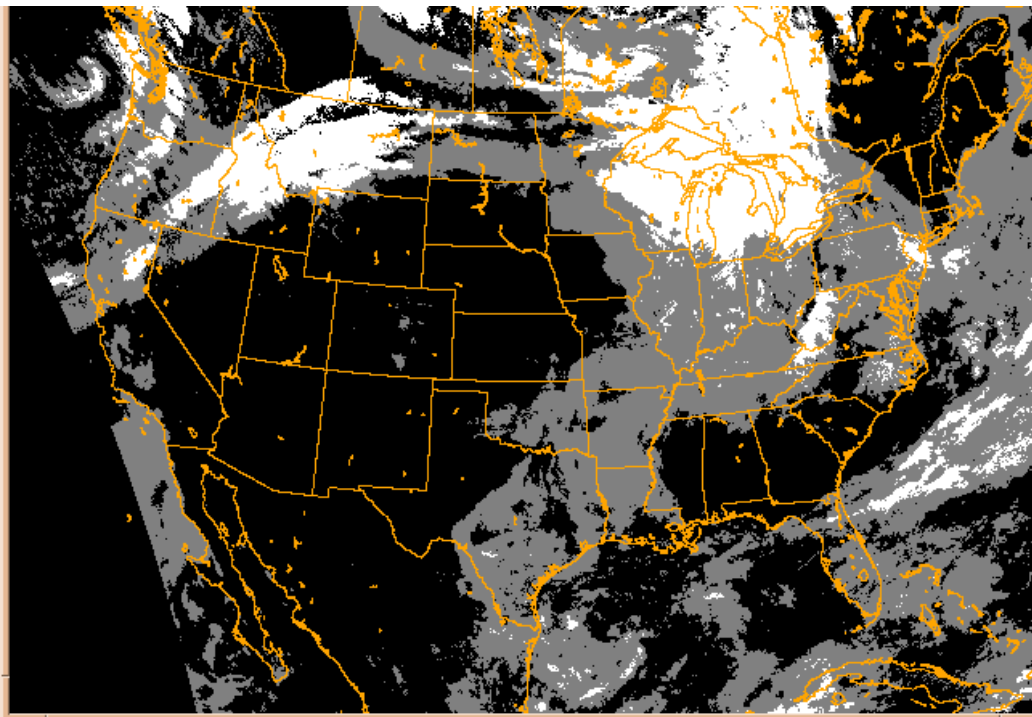


Figure 7. Cloud mask product valid at 1715 UTC on 19 November 2007. White areas denote ice-crystal clouds, grey denotes water-droplet clouds and black indicates no cloud detected. Data from GOES-12 in Lambert Azimuthal Equal-Area projection.

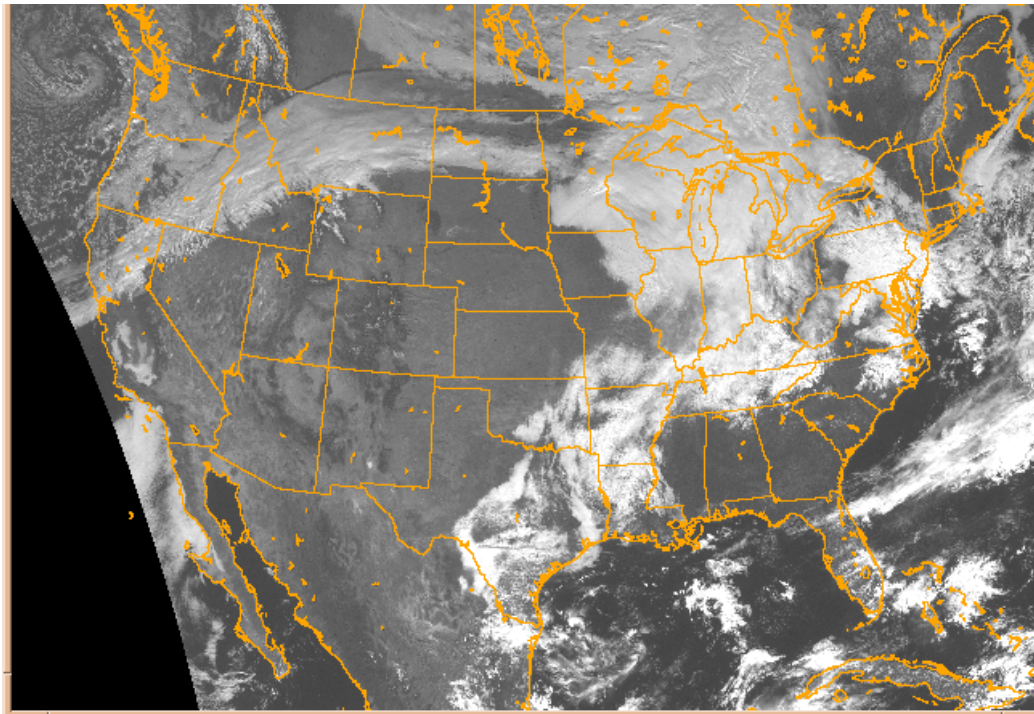


Figure 8. GOES visible channel image valid at 1715 UTC on 19 November 2007. Data from GOES-12 in Lambert Azimuthal Equal-Area projection.



Evaluation of the performance of the cloud mask over that past year has revealed a number of deficiencies in the current implementation. The first is limited to winter nighttime cases, in which some low cloud remains unclassified due to little or no signal evident in the GOES mid-wave IR channel. An experimental improvement to this limitation, based on the dynamic thresholding technique first introduced in the SERCAA program was recently implemented. The technique has contributed to a marked improvement in the analysis, filling-in pronounced "salt and pepper" areas and providing more realistic cloud decks when compared visually with the corresponding long-wave IR channel.

The second limitation within the cloud mask is the false classification of snow as cloud cover. From noted observations, the sudden transition from bare ground to snow-covered can alter the long-wave IR background temperature as much as 25K. Because the long-wave IR background field is generated from the most recent 15-day period, (in which the warmest pixel is selected as being representative of the background) the background classification procedure lacks the ability to detect abrupt brightness temperature moderation due to snow cover. Knowledge of the change from a snow-free to snow-covered background is an important first step in whether the long-wave IR background field can be adjusted to account for a significant change in background IR brightness temperature over a relatively short period of time. Snow cover will also impact the obvious bright cloud test, which depends on composite images that characterize the background based on low albedo clear-scene statistics. Obtaining daily snow cover maps will be a necessary first step towards addressing this limitation. In addition to the limitations mentioned above, the MIT/LL cloud detection algorithm exhibits degraded performance in the terminator region due to varying solar illumination across the region; and at night, when the visible channel is unusable and the mid-wave IR channel no longer has a reflected solar component that is so pronounced during daylight hours.

Despite deficiencies that are being addressed, the satellite cloud mask is now used in the national CIWS system for per-radar data quality editing. Currently, the MIT/LL national CIWS system is operational but the results are not yet displayed to

users who still use the legacy CIWS system. The national CIWS system extends the original CIWS domain of the northeast quadrant of the United States to the entire 48 contiguous states (CONUS coverage). It is anticipated that legacy users will have access to the improved national CIWS by the spring/summer of 2008.

Currently, the approach to using the satellite cloud mask for data quality editing is fairly cautious. The algorithm removes HRVIL and HREET data from the single radar products where there is no evidence of cloud in and around the area of return. The cloud mask is dilated a given amount (currently 20km) and, after the dilation, HRVIL and HREET data in areas away from the cloud are removed. Because the satellite cloud mask quality is better when it can incorporate visible data, and because of issues at the day/night terminator, satellite cloud mask data quality editing is applied only during daylight hours as determined by the solar zenith angle. This initially limits the ability to substantially deal with the onerous fair weather biological returns.

This satellite cloud mask data quality editing step is applied to each single-radar HRVIL and HREET product received from the ORPG as a first step in the CIWS per-radar processing stage. Figure 9 shows an example of satellite cloud mask editing. All the HRVIL data (upper left) in this example are erroneous (the spike and speckle editor were not run). The only edited data are away from cloud (non-blue areas, lower left) and where the solar zenith angle indicates daytime conditions exist. The upper right shows the edited result from application of the cloud mask technique. The lower right depicts the satellite data for reference.

The per-radar processing stage also includes tracking and trend detection. Because the satellite cloud mask data quality editing is applied at this early stage, the per-radar tracking and trending algorithms benefit from any data quality editing improvements made to the individual radar data. After the per-radar processing stage, mosaic creation algorithms merge HRVIL, HREET, and trend data from individual radars together into images. Mosaics of HRVIL and HREET are used to depict the location and intensity of weather as well as for input to forecasting algorithms.

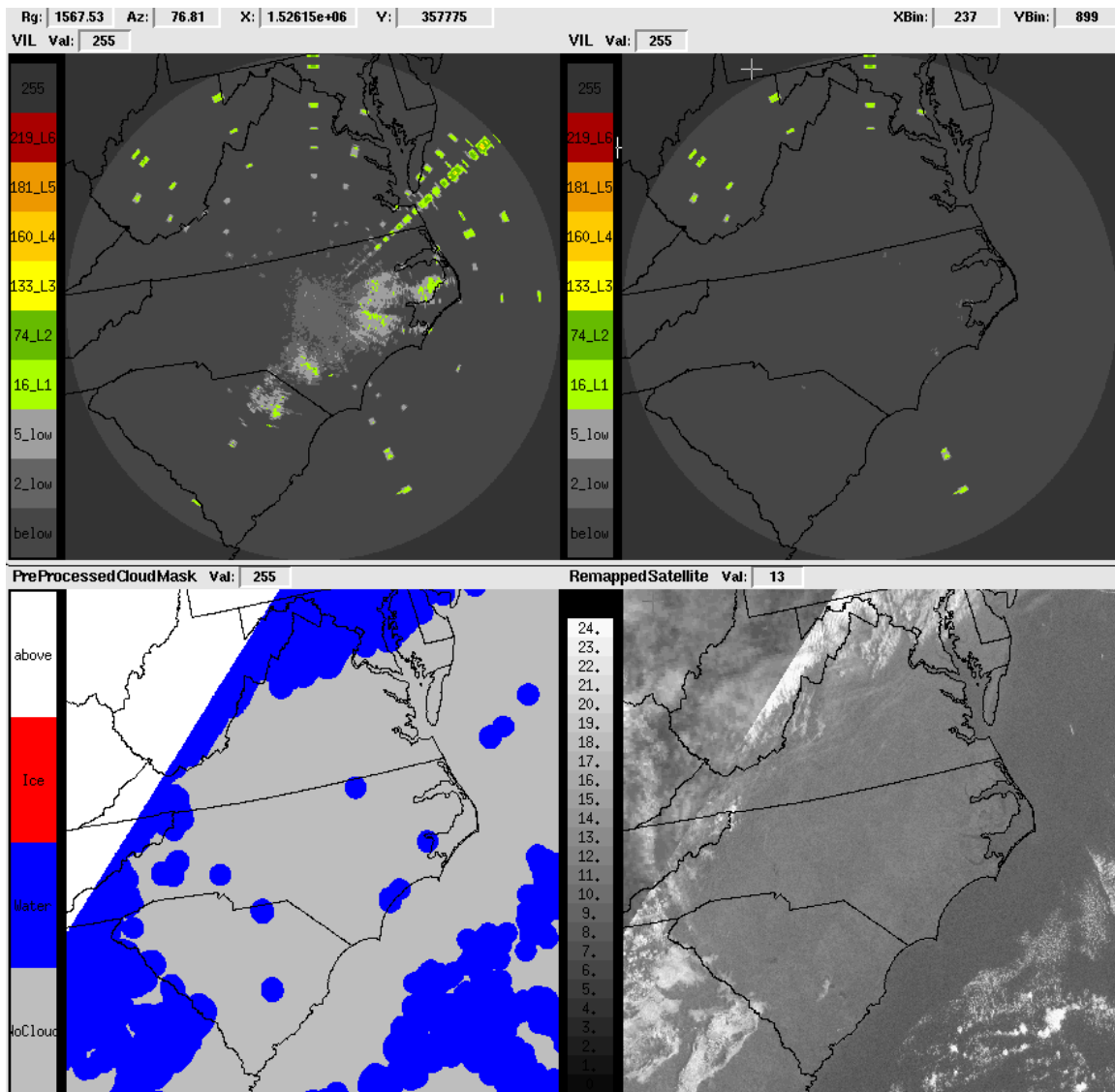


Figure 9: The upper left panel is HRVIL (in CIWS color scale) from the KRAX (Raleigh, NC) NEXRAD on Nov. 21, 2007 at 14 UTC before satellite cloud mask data quality editing is applied. The upper right is after the cloud mask editing is applied. Lower left is the dilated cloud mask (blue is cloud, gray no cloud, white where the solar zenith angle indicates not daytime). Lower right is the cloud (visible and IR remapped). Clutter is only removed where no cloud is nearby and daytime conditions prevail.

#### 4. MOSAIC DATA QUALITY

The CIWS mosaic creation algorithm merges HRVIL and HREET products from NEXRAD, TDWR, and Canadian radar data after the per-radar processing stage. Separate mosaics are created using different rules (described below). The MIT/Lincoln Laboratory legacy CIWS system utilizes data from 61 NEXRAD radars, 11 TDWR radars and 5 Canadian radars. The national CIWS system utilizes data from the same TDWR and Canadian radars and expands its coverage to include 135 NEXRAD radars. The national CIWS

mosaic algorithm is described here, but the mosaic algorithm is quite similar to that used with legacy CIWS.

Separate VIL and Echo Top mosaic products are created. Each point on the output grid (resolution 1 km) of each mosaic process is populated with one value chosen from a set of candidate values gathered from a number of overlapping, neighboring radar products. The number of available values in the set depends on the number of radars associated to each output grid point. The distance to the output grid point from each radar providing data to the set varies. It

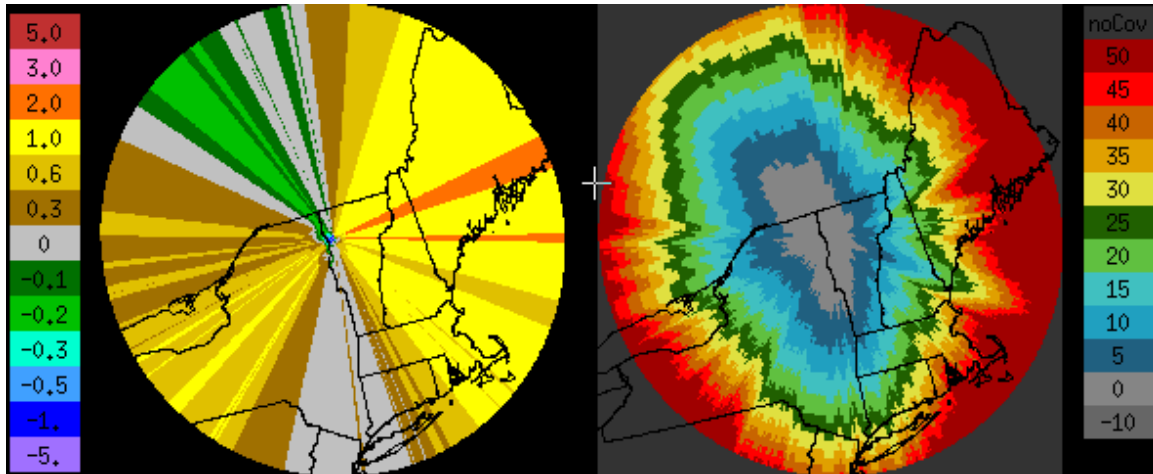


Figure 10. Beam blockage as computed for the KCXX NEXRAD radar. Left image shows the minimum non blocked elevation angle expected in degrees, and right shows the resulting altitude expected for a beam with minimum non-blocked elevation and range in kft.

is possible that only a single radar is associated to an output grid point.

It is important to know whether beam blockage is an issue for any points in the single-radar products. NEXRAD products do not provide information about beam blockage. The mosaic process utilizes a beam blockage map computed for each radar using terrain information associated with the radar location. The minimum non-blocked elevation expected under normal propagation conditions for a given range is computed. Where the minimum non blocked elevation exceeds the minimum elevation used in a volume, the HRVIL for a given radar is considered impaired due to possible beam blockage. Figure 10 shows an example of this for the KCXX radar in Burlington Vermont.

#### 4.1 VIL Mosaic Process

The overall mosaic strategy for the CIWS HRVIL mosaic is to select the “maximum plausible” value where possible. The intent is to ensure that the multiple-radar mosaic does not suppress regions that may only be observed by one radar (especially pertinent early on in the development of a convective cell), and to avoid unnecessarily reducing high HRVIL values as might occur if a mean or median filter were used. It also considers each radar input start time in an attempt to prevent discounting new growth not yet shown by other radars whose volume start times may be older.

In the CIWS system, the mosaic process triggers on a 2.5 minute clock strobe. The

individual radar data inputs to the mosaic process arrive asynchronously every 4 to 10 minutes. Before the mosaic is performed, each radar product is advected in time using storm motion data derived from a cross correlation process run on that radar's data. The duration of the advection spans from the product time (volume end time) to the mosaic trigger time, simulating a mosaic of inputs that have all just finished updating. Inputs that are too old (end times older than 15 minutes) are dropped from the mosaic creation process.

After advection, the HRVIL mosaic is assembled using the maximum plausible HRVIL value where possible for each output grid point. The maximum HRVIL value determined to be plausible is selected from the set of radars within a given distance threshold of the output grid point. Plausibility is a function of the values observed by the other radars according to a set of thresholds and geometry considerations. The nominal distance threshold used is 230 km range for NEXRAD radars. The 230 km range was selected because, at that range, the NEXRAD's lowest 0.5 deg tilt elevation angle scan is expected to have reached over 5 km in altitude. Beyond that range the radar is more likely to miss lower levels of storms thus underestimating the overall intensity (artificially reduced HRVIL). If no radar is within the nominal distance to the output grid point, or if all the radars within the threshold distance are impaired in some way (possible attenuation, beam blockage, etc), the maximum available HRVIL value is selected. When one radar without discounting issues is within the desired range, that radar's HRVIL value is used. Otherwise the

maximum plausible logic is used to select a value from the set of HRVIL values of radars within the threshold distance of the output grid point location.

The plausibility process begins by first examining the highest HRVIL value from the set associated to an output grid point location. If that highest HRVIL value is below threshold, it is used without further checking. Otherwise the value is compared to those determined by the other radars in the set. The value is used if the highest HRVIL value is confirmed by at least a given percentage (set to 40%) of the remaining radars in the set that have the ability to confirm (described below). If no radars in the set have the ability to confirm, the highest value is used. Otherwise if the highest value cannot be confirmed by the required percentage, the value is found to be suspicious. If the value is suspicious, and persistence requirements are met, the value is thrown out of consideration, and the next highest value is

examined against the remaining radar values in the set using the same logic. This procedure is repeated until a result is found.

A necessary condition for a radar to be in a position to confirm is that the location being confirmed (output grid point) is within a given "sweet spot" range (35 km to 230 km for NEXRAD radars) from the potential confirming radar location. The potential confirming radar also cannot be considered impaired at that location due to possible beam blockage or, for TDWR data, due to possible attenuation or range fold editing. In addition, a confirmation threshold must be found based on the HRVIL value under test, the distance of the output grid point (pixel in the product image) to the radar with the HRVIL value under test, and the distance to the potential confirming radar. Figure 11 graphically shows how the confirmation threshold is found.

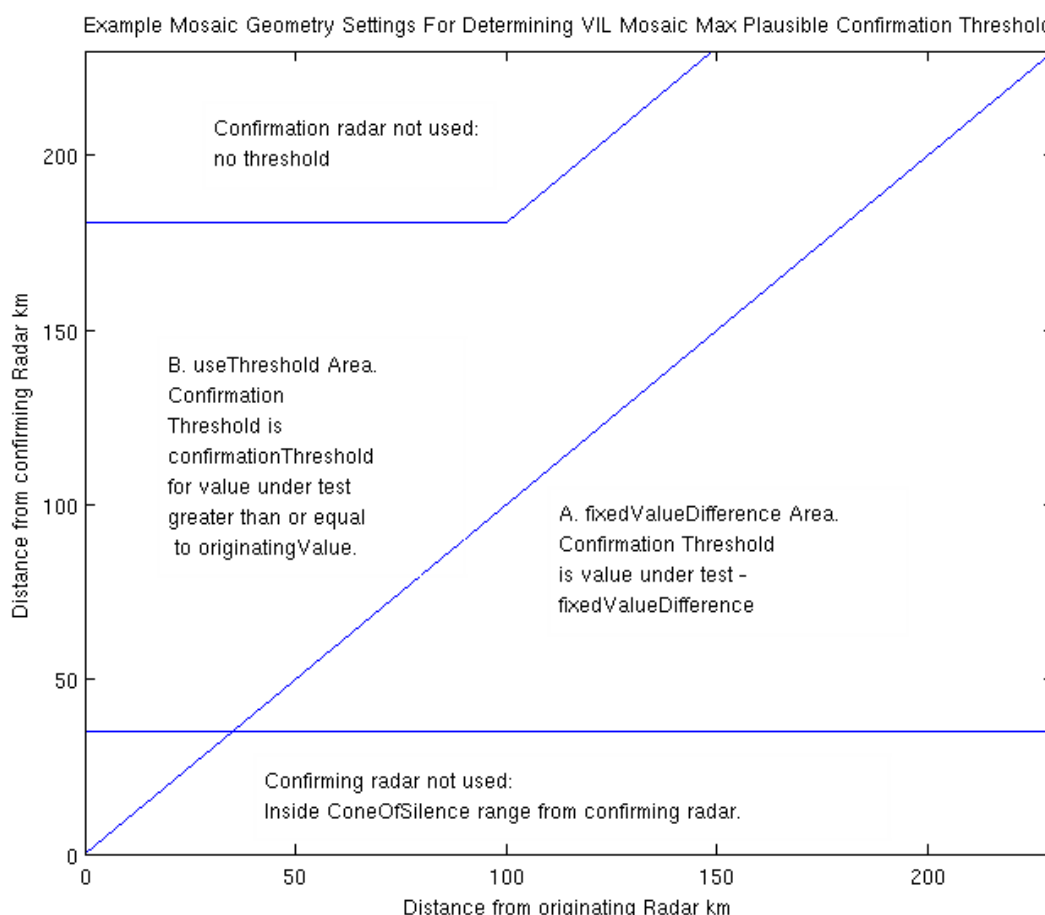


Figure 11. The threshold used in the maximum plausible logic to confirm a test HRVIL value from the originating radar using data from a confirming radar depends on the distances from the radars and the test value. In the area labeled A in the image, the value is a threshold equivalent to 15 dBZ less than that of the test value. In section B, values exceeding the equivalent of 30 dBZ may be edited if the confirming radar's value is less than 10 dBZ.

If these conditions are met, and a confirmation threshold is found, the confirmation radar data are searched for pixels at or above the required confirmation threshold. The search area is +/- three pixels from the point location in the confirmation radar data. In order for the point to be confirmed all the confirming radar HRVIL values in the search area must be valid (within coverage, not flagged for possible attenuation, beam blockage or range fold editing), and a given percentage of the values searched must be at or above the confirmation threshold (currently set so 1 point in the search can confirm the value). If invalid HRVIL values are encountered in the search, the radar is reclassified as disqualified as a confirming radar for this point. Otherwise, the radar is considered able to confirm the value and the result of whether it did or did not is used to help decide whether the test value should be used, or considered suspicious and possibly rejected.

A value judged inconsistent with respect to the confirming radars (i.e. - a suspicious value) can still be used in the mosaic. A note is made that the value is suspicious at this time for that radar. The value must still pass a persistence check before it is rejected from the mosaic. The persistence check is designed to guard against editing growing weather that has not yet appeared in other radar data.

For the persistence check, one of the following two persistence tests must be met for the value to be removed from consideration. For the first test, if the only radars in the set being considered have start times later than the start time of the radar whose HRVIL value is under test, the value would be still considered suspicious by those radars. In this case it is assumed that since the value is not

confirmed by more recent radars it is probably not a new storm. In the second test, a search of points around the point location is conducted to determine if there is a point previously labeled suspicious in the test radar's last volume scan. In this case, the suspicion in the area is not new for the radar, and the suspicious test value is permitted to be thrown out.

Despite improved data quality of individual HRVIL and HREET products and application of the satellite cloud mask technique, the radar data may still contain clutter causing the value of the set to be false. The HRVIL mosaic process attempts to filter out those anomalous returns where possible using data from neighboring radars that have a sufficiently good view over the output grid point, resulting in a high fidelity maximum plausible HRVIL value. Figure 12 is an example of the maximum plausible logic successfully rejecting the high HRVIL seen along the southwest tip of Lake Michigan associated with AP from the KGRR (Grand Rapids, MI) NEXRAD. It is rejected in the mosaic since it is not confirmed by returns from the KLOT (Chicago, IL) and KMKX (Milwaukee, WI) radars.

Figure 13 shows an example of the VIL mosaic in the national CIWS system. This result (upper left) is a product of the single-radar product generation followed by per-radar processing, the application of the satellite cloud mask (lower left), and the maximum plausibility logic during mosaic creation. The upper right panel shows that beam blockage out west (yellow) may be problematic. The black regions show where the cloud mask provided additional editing. The lower right panel shows the corresponding satellite image.



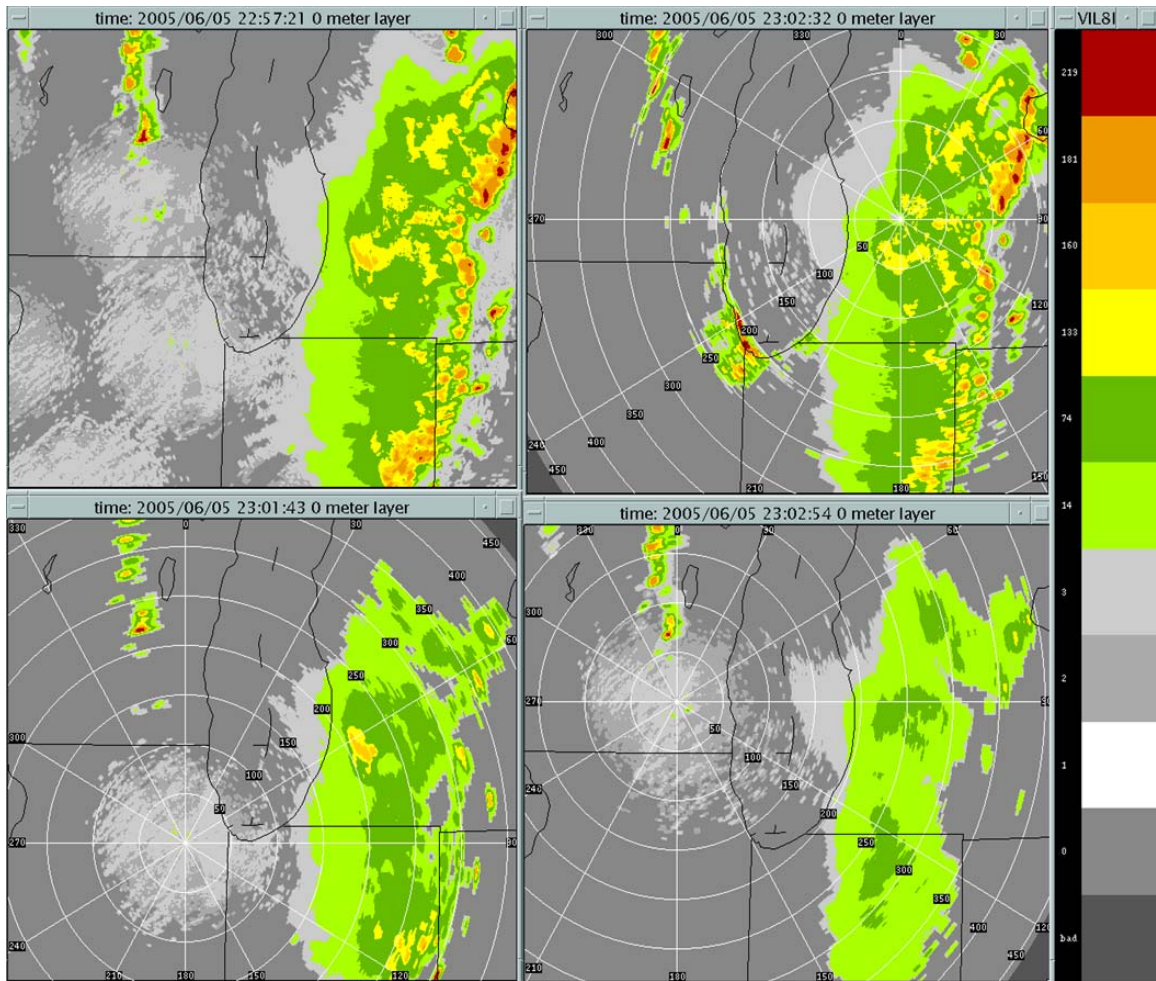


Figure 12: Top left is VIL mosaic, top right is the KGRR input, bottom left is the KLOT input, bottom right is the KMKX input. The high returns found in the KGRR VIL are not in KLOT or KMKX and are not used in the mosaic due to the maximum plausible logic. On the individual radar images, range rings originate from the radar location at 50 km intervals.

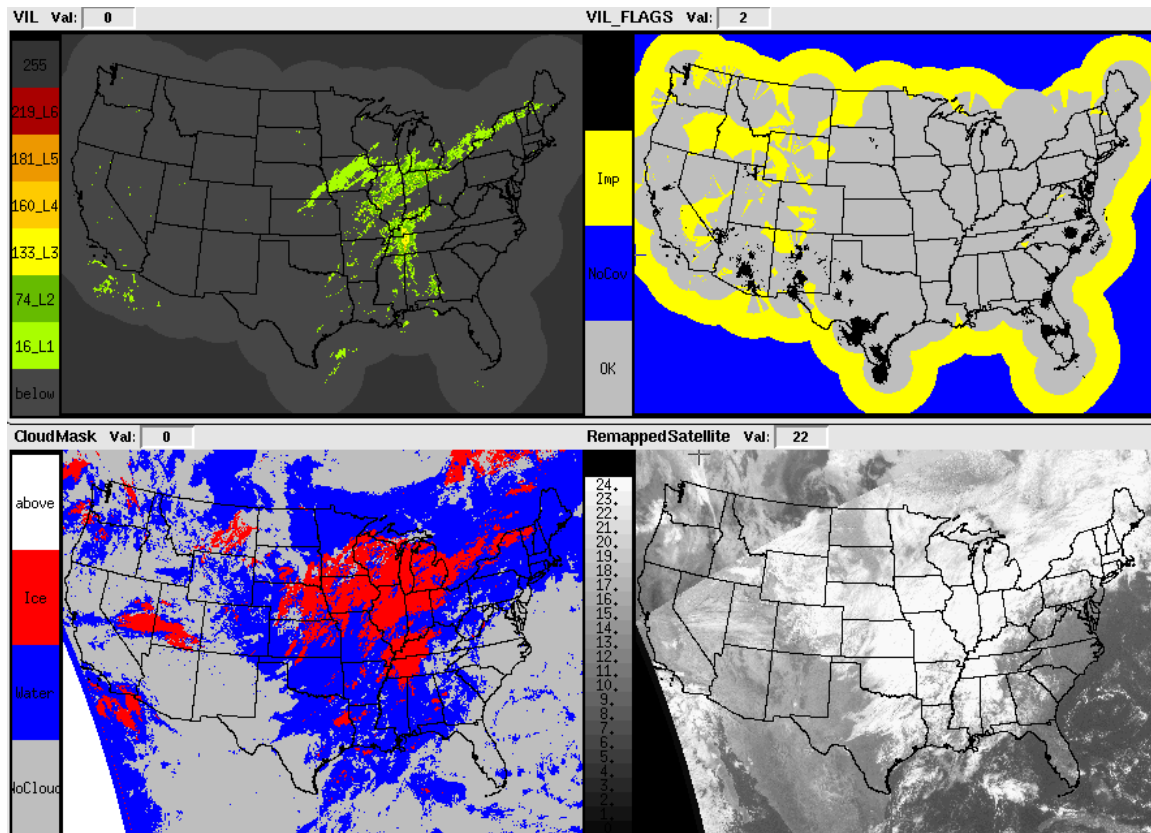


Figure 13: Top left is the VIL mosaic from Nov. 21, 2007 at 16:45 UTC; Top right is the VIL mosaic flags (blue no coverage, yellow impaired due to long range or possible beam blockage, black where satellite cloud mask editing took place); bottom left is the cloud mask; and bottom right is remapped satellite IR and visible data.

## 4.2 Echo Top Mosaic Process

The HREET mosaic logic is straight forward relative to the HRVIL mosaic logic. In locations where there are multiple HREET input values, the program uses the highest possible value, unless that radar's corresponding HRVIL value was rejected earlier by the maximum plausible HRVIL mosaic logic. In that case, the highest HREET value available at that location that is not associated with a rejected HRVIL value is used. If the selected HREET value is topped, the echo top mosaic is flagged topped as well at that location. A topped echo top occurs when the 18 dBZ threshold is met or exceeded at the highest elevation tilt angle of the radar volume available for a given range from the radar.

Finally, at the mosaic stage, a final cross check of the HREET mosaic values against the HRVIL mosaic values is performed. The test checks that echo top values above a given altitude have sufficient associated HRVIL such that the echo top estimate is likely to be valid. If a HRVIL

value is too small, the echo top mosaic value is edited (removed).

## 5. SUMMARY

Removing non-weather returns from the precipitation and echo top data is particularly important for the CIWS system where automated tracking, trending and forecast algorithm results can be degraded by non-weather returns. As described in this paper, the CIWS system has begun applying a mounting evidence data quality classifier technique. This technique relies on data quality checks and interventions at various stages of the process leading to high fidelity products of weather location and intensity used by FAA aviation weather systems.

The concept of using mounting evidence is at an early stage with the first application being incorporation of satellite cloud masking during daytime conditions. As the concept matures, additional levels of evidence will be introduced. This should include incorporation of surface

observations and model data grids. Sophisticated “situationally applied” rules will be developed that allow for more aggressive data quality editing but restrained to certain circumstances. With additional input of levels of evidence, a weighting scheme tied somewhat to situational application will be introduced.

Additional data quality initiatives will continue to be pursued concerning the individual radar products, per-radar processing, and satellite cloud masking capabilities, and the use of intelligent mosaic practices. The addition of more radar products such as NCAR’s Radar Echo Classifier and an HRVIL first-tilt-only flag product may bolster aspects of the per-radar processing. Also, the NEXRAD network will be upgrading to a dual polarization capability beginning late 2009. The potential from that will be improved data quality through the ability to classify hydrometeors. That classification may be used further to improve the HRVIL and HREET products. Additionally, beam blockage may be mitigated to some extent through use of new dual polarization parameters.

## **6. REFERENCES**

Jedlovec, G.J., and K. Laws, 2003: GOES Cloud Detection at the Global Hydrology and Climate Center. Preprints 12th Conference on Satellite Meteorology and Oceanography, Long Beach, CA, AMS.

Gustafson, G.B., R.G. Isaacs, R.P. d’Entemont, J.M. Sparrow, T.M. Hamill, C. Grassotti, D.W. Johnson, C.P. Sarkisian, D.C. Peduzzi, B.T. Pearson, V.D. Jakabhazy, J.S. Belfiore, and A.S. Lisa, 1994: Support of Environmental Requirements for Cloud Analysis and Archive (SERCAA): Algorithm Descriptions. PL-TR-94-2114, Phillips Laboratory, Hanscom AFB, MA. ADA-PL-283240, 100 pp.

d’Entremont, R. P., and G. B. Gustafson, 2003: Analysis of Geostationary Satellite Imagery Using a Temporal-Differencing Technique. *Earth Interactions*, **7**, 1-25.

Howard, Ken, NSSL, personal communication.

Smalley, D.J. and B.J. Bennett, 2002: Using ORPG to Enhance NEXRAD Products to Support FAA Critical Systems. 10th Conference on Aviation, Range, and Aerospace Meteorology, Portland, OR, American Meteorological Society, paper 3.6.

Smalley, D.J., Bennett, B.J., and M.L. Pawlak, 2003: New Products for the NEXRAD ORPG to Support FAA Critical Systems. 19th Conference on IIPS, Long Beach, CA, American Meteorological Society, paper 14.12.